RoboSub 2026 Technical Design Report
Universidade de Brasília (Team All Blue)

André A. Flamínio, Andrei B. F. M. Gaspar, Artur F. Gonçalves, Daniel A. R. Pinto, Gabriel O. P. Mendes, Gabriella K. A. Silva
Giovanni N. Catelli, Gustavo R. B. Albuquerque, Henrique A. P. Portela, João Pedro O. G. Pereira, João Victor S. Santos,
Leandro B. Carvalho, Marcus V. S. Berlanda, Matheus M. Perdoncini, Pedro B. T. Castro, Sophia M. Oliveira

***Abstract*—For RoboSub 2026, Team All Blue continued the development of our second AUV, Peixonauta, with a focus on robustness and reliability by addressing the weaknesses of the previous season. The AUV is equipped with seven thrusters, and its control system was updated from a Cascade Control architecture to a desired acceleration loaded direct in the motors for greater stability. The electrical system was redesigned for modularity, robustness, and reliability to ensure the AUV can complete the circuit. This upgrade enables advanced perception using the YOLO26n neural network for object detection and RTAB-Map for SLAM. The mechanical design was refined through topology optimization, and mission logic is managed by a modular Behavior Tree structure.**

I. Competition Strategy

For RoboSub 2026, the All Blue team's strategy centers on maximizing mission completeness during the inaugural competition site run of our second AUV, Peixonauta. Shifting from previous conservative approaches, we are now explicitly focused on successfully executing all tasks up to the Advanced scoring tier—encompassing both Core and Advanced objectives. To achieve this ambitious goal despite existing sensor limitations, our mission logic is governed by a highly modular Behavior Tree (BT) structure. This intelligent architecture is designed to systematically sequence tasks and dynamically adapt to environmental feedback, ensuring the AUV can reliably navigate the circuit and maximize its score without failing mid-run.

This aggressive software strategy is fully supported by critical hardware and control refinements aimed at unmatched reliability. Peixonauta's mechanical design features topology optimization and a streamlined seven-thruster configuration that, when paired with a newly implemented Cascade Control architecture, provides exceptional stability during delicate maneuvers. Furthermore, a redesigned, modular electrical system reliably powers our upgraded compute platform, allowing us to fully leverage advanced perception tools. By utilizing the YOLO26n neural network for precise object detection and RTAB-Map for robust SLAM, the AUV possesses the processing power and environmental awareness necessary to confidently tackle the advanced circuit.

1) Enter the Pacific — Gate: The first task will be the gate. The AUV begins its run after accepting the coin, which randomizes its initial orientation. It then submerges and initiates a local scan with its stereo camera until it detects the gate using the neural network. Upon detection, the visual servoing system is activated to position the AUV in the ideal pose. This position facilitates more precise recognition of the images on the gate, allowing for the correct choice of side to pass through based on whether the reef shark is to the right or left of the red marker.

2) Navigate the Channel (Slalom): The strategy for this task depends on the side chosen when passing through the gate. The AUV must keep the red pipes consistently on the same side (either right or left) while navigating within the channel formed by the vertical pipes. Navigation control is managed by visual servoing, supported by color recognition to ensure the AUV remains within the designated area and follows the correct path.

3) Recon (Dropper): For the Recon task, the AUV utilizes its bottom-facing camera and the YOLO26n neural network to scan the 3D PVC pipeline and visually classify the target bins based on their role-specific vinyl prints. Once the correct bins are identified, the Behavior Tree logic transitions the vehicle into a highly precise alignment phase. By leveraging our Cascade Control architecture for stable horizontal station-keeping and depth management, the AUV positions itself safely above the targets, maintaining close proximity to minimize collision risks with the pipeline structure. This precise positioning guaranties accurate deployment of our two markers into the designated bins, successfully securing the Advanced scoring objectives for this mission.

4) Dropper Torpedos (Tagging): To guide the AUV to the torpedo task, pingers will be used. With the aid of the front-facing cameras, the AUV will position itself in front of the task panel. The objective is to align the firing line with the targets (the openings in the panel) while maintaining an appropriate distance to ensure both visibility and firing accuracy. The computer vision algorithms and firing system were designed to guarantee at least two hits on the available targets.

5) Octagon (Ocean Cleanup): The strategy for this task is to center the AUV within the octagon using the collection table as a reference. The focus will be on collecting the bottles on the table using the gripper. After collecting each object, the AUV will surface and deposit the item into the corresponding basket. If time is running out, this will be the final task attempted.

6) Return to Gate (Return Home): Upon completing the tasks, the AUV will use the data gathered during mapping (SLAM) to plot a return route to the starting gate. The route will be defined by taking obstacles into account, aiming to minimize any risk of collision and ensure safe navigation to the final point.

II. Design Strategy

A. Mechanical Subsystem

1) Stereo camera hull: For the new stereo camera (Luxonis OAK-D S2), integrated into the AUV to provide more accurate depth perception through stereoscopic vision, we developed a rectangular watertight hull. It was machined from 6061-T6 aluminum alloy, designed for use with a 120 × 3 mm O-ring and a 6 mm thick solid polycarbonate lid. Additionally, internal and external 3D-printed mounts were developed: the internal mount secures the camera inside the hull and prevents movement during operation, while the external mount attaches the hull to the AUV frame.

2) Floaters: To correct the vehicle's buoyancy and achieve neutral trim, two custom floaters were designed and fabricated. Each floater consists of an EPS foam core (density $\approx\ 20\,kg/m^3$) with dimensions 35 cm × 14 cm × 17 cm, resulting in a total displaced volume of approximately 16.5 liters. The polystyrene cores are sealed with a pure epoxy primer and then laminated with two layers of $200\,g/m^2$ E-glass fabric impregnated with epoxy resin. This composite skin provides a rigid, waterproof shell that prevents water absorption while adding minimal mass. The two floaters are positioned symmetrically on the outside of fairing, more especially on the sides, and their combined buoyancy offsets the excess weight of the vehicle, ensuring a neutral flotation at any operational depth.

3) Cable Management: The cable management system of the AUV was redesigned and improved to enhance safety, reliability, accessibility, and overall system organization. By properly routing and securing the cables, the risk of loose connections, electrical interference, and mechanical damage caused by vibration, movement, or water exposure was significantly reduced. The improved organization also facilitates maintenance and troubleshooting, allowing faster access to critical components during testing and competition. In addition, a cleaner and more structured internal layout improves assembly consistency and reduces the likelihood of human error during integration. Beyond the technical advantages, the enhanced visual presentation reflects a higher level of engineering professionalism and system quality.

4) Torpedo: The development of the new torpedo focused on reducing its size without compromising firing efficiency. A CO_2 cylinder is externally triggered by springs housed in a 3D printed compartment. The springs are attached to a small iron rods that come out of the 3D printing support piece of furniture. The part where they are attached is stretched and held by a small lever mechanism and later released by a solenoid, driving a pin that punctures the cylinder, releasing gas to propel the torpedo. The torpedo body is also 3D-printed and was fitted with ballast to adjust its density and buoyancy. Compared to the previous model, the new mechanism is significantly smaller and more practical for maintenance and transport.

B. Electrical Subsystem

A critical assessment of the previous competition cycle revealed several limitations in the electrical subsystem that directly impacted the reliability and operational robustness of Peixonauta. One of the primary issues identified was the lack of reliability in the sealing system of the battery enclosure, which introduced significant risks to system safety and long-term operation in submerged environments. In addition, the ESC control board exhibited intermittent failures during validation tests. As the root cause could not be conclusively identified within the available development timeline, the team adopted a strategic redesign approach to ensure vehicle operability and reduce integration risks before the competition phase. Furthermore, the internal layout of the control cylinder was revised to improve space utilization and thermal distribution. This redesign was motivated by the increasing subsystem density inside the enclosure and the need to mitigate localized heat accumulation, improving maintainability and overall system stability during extended operation.

1) Internal Organization: For the 2026 season, the overall electrical architecture of Peixonauta was preserved, as the previous design demonstrated satisfactory performance in terms of thermal dissipation, space optimization, and system maintainability. The vehicle continues to employ a dual pressure-hull configuration, with one enclosure dedicated to power distribution and actuator driving systems, while the second enclosure is dedicated to control and computation subsystems.

2) Battery System: Due to the limited reliability of the previous battery enclosure sealing system, the team decided to reuse the battery pressure hull originally developed for Iara, the team's 2024 AUV platform. This decision reduced integration risks while leveraging a previously validated mechanical solution with proven operational reliability. As a consequence of this redesign, the power architecture was also simplified compared to the previous iteration. The system now employs a 5 Ah LiPo battery pack with a nominal voltage of 18.5 V, featuring an integrated Battery Management System (BMS) responsible for overcharge and overdischarge protection.

3) Power Cylinder: The actuator electronics architecture preserves the same modular approach adopted in previous iterations, consisting of two primary boards: the Power Management Board (PMB), responsible for power distribution and regulation, and the ESC Backplane Board, dedicated to actuator driving integration. However, during electrical subsystem validation tests, the original ESC Backplane Board exhibited intermittent and non-reproducible failures, preventing accurate root-cause identification within the available development timeline. To mitigate integration risks and maintain vehicle operability, the team adopted a contingency redesign strategy based on the direct integration of standalone ESC modules. This decision enabled the continuation of vehicle development without compromising the reliability of the actuation subsystem during the competition preparation phase. Nevertheless, investigation of the original board failure mechanisms remains an open development point for future design iterations.

The Power Management Board (PMB) was preserved without major modifications from the previous season, as it demonstrated stable and reliable operation throughout validation and in-water testing phases. The PMB is responsible for voltage regulation and power distribution across the vehicle's electrical subsystem. Starting from the battery supply voltage of 18.5 V, the PMB generates regulated 18.0 V, 12.0 V, and 5 V power rails, which supply the ESCs and thrusters, the Jetson Orin and Pixhawk flight controller, and the onboard cameras, respectively. An ESP32 microcontroller continuously monitors battery status in real time and manages the integrated kill switch system implemented directly on the board. When activated, the kill switch immediately disables power delivery to the vehicle, ensuring operational safety during testing and competition procedures.

4) Control Cylinder: The hydrophone acquisition board was redesigned with a narrower 25–40 kHz passband using an 8th-order Butterworth filter, providing sharper cutoff characteristics and improved passband stability. This redesign enabled more selective filtering targeting the acoustic frequencies relevant to the competition environment. The signal amplification stage was also increased by 20 dB to improve output signal quality and increase signal-to-noise ratio during acoustic acquisition. Additionally, the ADC was upgraded to the AD7928BRUZ, enabling simultaneous sampling of four channels at 250 ksps per channel. This modification provides the temporal resolution required for more accurate acoustic source localization.

The control support board has been redesigned to accommodate the current system hardware. The new layout integrates the Jetson Orin, the Pixhawk flight controller, and two regulated power buses, operating at 12.0 V and 5.0 V, respectively. The 12.0 V bus is responsible for powering the Jetson Orin and three solenoids dedicated to the dropper and torpedo actuation mechanisms, while the 5.0 V bus is used exclusively to power the onboard camera. This reorganization results in optimized space within the control cylinder.

Onboard sensors play a fundamental role in the AUV's performance during competition. This season, Peixonauta features two IMUs (inertial measurement units) and four hydrophones. The first IMU is integrated into the camera (OAK-D S2), being used to assist the visual odometry process performed by the camera itself, contributing to the estimation of the vehicle's position. The second IMU is integrated into the Pixhawk flight controller, whose function is to correct the inertial readings and republish them at a higher frequency, ensuring greater precision and responsiveness to the navigation system. Both devices are connected directly to the Jetson Orin power ports. The four hydrophones are responsible for the acoustic detection and location of the pinger for the competition tasks, being powered by the 5.0 V bus.

C. Software Subsystem

1) Simulation Environment: For this year's simulation environment, the team's approach was to continue with the previous consolidated system, based on the integration between Unity, used for high-fidelity 3D visualization, and ROS (Robot Operating System)[18], which is responsible for the control structure, publication of sensor data, and execution of algorithms.

In the current edition of the competition, the simulation environment was redesigned and updated to Unity version 6.4, aiming for higher visual fidelity and a more precise validation of the algorithms against real-world tasks. Additionally, all mission-related objects were remodeled and re-textured from scratch to faithfully reflect the competition's current setup. Consequently, the representation of the pool and the task elements ensures a superior level of realism and accuracy for the vehicle's testing phase, thereby reducing the sim-to-real gap and making software validation in the virtual environment more predictive of actual competition performance.

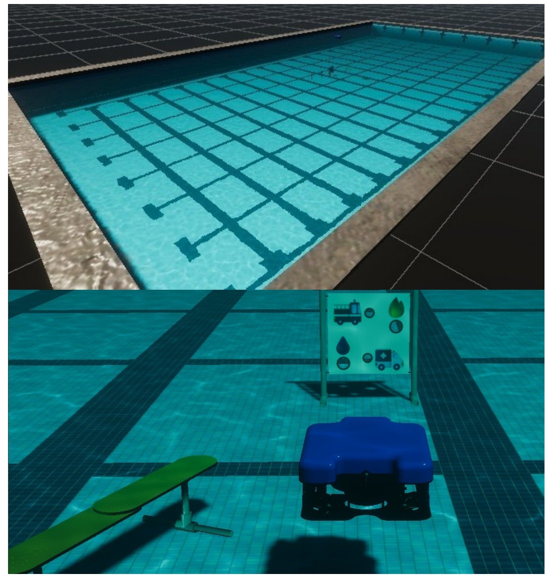

Fig. 1. Updated simulation environment developed in Unity 6

2) Computer Vision: When it comes to object detection, significant improvements were made in both the neural network and color detection algorithm [10]. The neural network was upgraded from the YOLOv5 nano architecture to YOLO26 nano, aiming to optimize processing accuracy and speed, as it is an improvement made by Ultralytics in this new architecture. Furthermore, the new version integrates the use of CUDA cores from the Jetson platform, enabling parallel processing for the neural network. Regarding color detection, the methodology was refined to identify only one object at a time, resulting in higher stability when detecting 'Paths' — elements that demand continuous monitoring and feature high-contrast colors. Additionally, the method for calculating the object's vertices was modified to increase the stability of these points and improve the Visual Servoing system.

Finally, the Visual Servoing system was enhanced to utilize four reference points in estimating the object's position, in addition to an Extended Kalman Filter (EKF) that acts with the Visual Servoing to improve accuracy. Moreover, the new implementation enables these references to be obtained through both methodologies: via the neural network as well as through color detection.

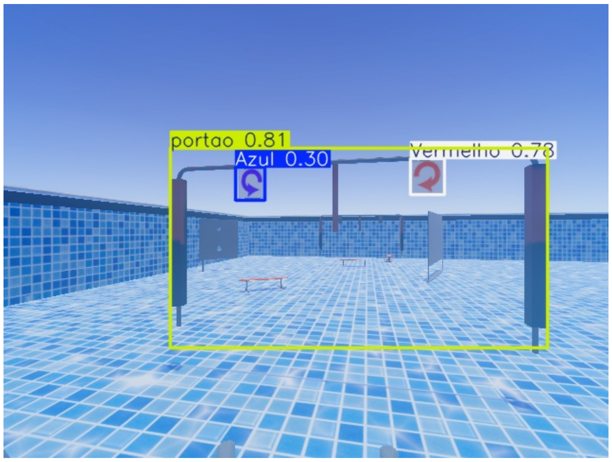

Fig. 2. Early object detection test using YOLO26 in the old simulation environment

3) Camera Upgrade: In the current edition of the competition, the AUV underwent an upgrade to its vision system with the replacement of the main camera, the new OAK-D S2 by Luxonis. The new technology allowed for more efficient frame synchronization and features native visual odometry packages for vehicle mapping and positioning. To optimize the reliability of the estimated states, these data were integrated with those from the AUV's internal Inertial Measurement Unit (IMU) which is from the PixHawk with ArduSub firmware installed. This sensor fusion was performed using the *robot_localization* package, significantly increasing the accuracy of position, as well as linear and angular velocity measurements.

4) Control subsystem: Building upon the Cascade Control (CC) architecture introduced in the previous cycle, three principal developments characterize this year's control system: a correction of the thruster allocation matrix, an enhancement to the control law with direct acceleration allocation, and the integration of a reactive obstacle avoidance module. Thruster Allocation Matrix Correction. The 67 thruster allocation matrix, which maps body-frame forces and torques to the individual effort commands of the seven thrusters as a function of their mounting positions and thrust direction vectors, has been corrected based on updated geometric measurements. The previous matrix contained inaccuracies that manifested as steady-state tracking errors, particularly in the roll and yaw channels. The corrected matrix is expected to improve trajectory-following precision across all six degrees of freedom.

1) *Control Law Enhancement and Direct Acceleration Allocation:* A new feedforward term has been introduced into the system's control law, and the computed acceleration commands are now allocated directly to the thrusters, superseding the previously employed *cascade_velocity_controller* ROS node. This modification simplifies the control pipeline by eliminating an intermediate processing stage and reduces the system's sensitivity to parametric uncertainties arising from dynamic modelling inaccuracies inherent to the CC framework. By operating on acceleration rather than velocity references, the controller achieves greater robustness against external environmental perturbations — such as unmodelled flow disturbances — without increasing architectural complexity.
2) *Reactive Obstacle Avoidance:* A reactive obstacle avoidance module has been integrated into the control framework, operating autonomously from the global path planner. The module employs the Deformable Virtual Zones (DVZ) algorithm [9] to generate a supplementary control law that is additively composed with the existing trajectory-tracking law. This formulation allows the vehicle to respond to unforeseen obstacles in real time while preserving convergence toward the planned trajectory when the obstacle-induced perturbation subsides, without requiring re-planning at the mission level.

5) Graphical User Interface: A dedicated Graphical User Interface (GUI) was developed as a significant addition relative to the previous year's system. The GUI consolidates real-time vehicle telemetry into a single operator station, displaying state estimates for position, altitude, and orientation, live feeds from the onboard cameras, battery charge level, and mission execution status. This centralised monitoring capability substantially reduces operator cognitive load during poolside testing and precompetition checks, providing immediate situational awareness without requiring direct interaction with the underlying ROS topic infrastructure.

Beyond passive monitoring, the GUI exposes a ROV teleoperation interface through which operators can manually command the vehicle via a joystick controller. Joystick inputs are interpreted by the interface and transmitted to the vehicle over the ROSBridge WebSocket connection, where they are consumed by a ROS node, responsible for allocating PWM to the motors, as direct acceleration commands. This interface, while not strictly obligatory for the competition, is extremely useful for the development phase and also for the competition itself.

Acknowledgment

We would like to express our deepest gratitude to the Universidade de Brasília and our two mentors, Professor Hugo Tadashi Muniz Kussaba and PhD candidate Leonardo Botelho Cardoso, for all their support and infrastructure. A special thanks to our former members, Eduardo Rossi, Rian Rocha, Pedro Matos, Wesley Oliveira and Professor Geovany Araújo Borges, for their shared knowledge and guidance, and to our colleagues from the competition teams with whom we share the workshop space, for the collaboration and camaraderie.

Bibliography

[1] Martin Philip Bendsoe and Ole Sigmund. *Topology optimization: theory, methods, and applications*. Springer Science & Business Media, 2013.

[2] Henry T. Brown. *Five Hundred and Seven Mechanical Movements*. New York, 1871.

[3] Cadence Design Systems. *High-Power PCB Design Considerations*. Accessed: 2025-06-30. 2021. URL: https://resources.pcb.cadence.com/blog/2021-high-power-pcb-design-considerations.

[4] B. Gabriel and D. Silva. *Low-Cost Embedded Linear Actuator*. https://repositorio.utfpr.edu.br/jspui/bitstream/1/31630/1/atuadorembarcadobaixocusto.pdf. Accessed: June 29, 2025. n.d.

[5] J. Gallardo-Lozano et al. "Battery equalization active methods". In: *Journal of Power Sources* 246 (2014), pp. 934–949. DOI: 10.1016/j.jpowsour.2013.08.026.

[6] David Halliday, Robert Resnick, and Jearl Walker. *Fundamentals of Physics: Electromagnetism*. 10th ed. Vol. 3. Rio de Janeiro: LTC, 2016.

[7] Hermann A. Haus and James R. Melcher. *Electromagnetic Fields and Energy*. n.d.

[8] Robert C Juvinall and Kurt M Marshek. *Fundamentals of machine component design*. John Wiley & Sons, 2020.

[9] John Muñoz et al. "Deformable Virtual Zone and Particle Filters Applied to Obstacle Avoidance in Mobile Robotics". In: *2016 XIII Latin American Robotics Symposium and IV Brazilian Robotics Symposium* (Oct. 2016), pp. 205–210. DOI: 10.1109/LARS-SBR.2016.41.

[10] Agneya Pathare. *Color Detection Using Python and OpenCV*. Accessed: 2025-06-30. 2024. URL: https://agneya.medium.com/color-detection-using-python-and-opencv-8305c29d4a42.

[11] Klaus Pohl. *Requirements engineering fundamentals: a study guide for the certified professional for requirements engineering exam-foundation level-IREB compliant*. Rocky Nook, Inc., 2016.

[12] *RTAB-Map ROS - Noetic and Newer*. *ROS Wiki*. http://wiki.ros.org/rtabmap-ros/noetic-and-newer, [Accessed: Jun. 29, 2025].

[13] Daniel J. Shanefield. *Solenoid Engineering Handbook*. n.d.

[14] Joseph Edward Shigley, Charles R Mischke, and Richard G Budynas. *Shigley's Mechanical Engineering Design*. 9th ed. McGraw-Hill, 2011.

[15] Joseph Edward Shigley, Larry D Mitchell, and H Saunders. "Mechanical engineering design". In: (1985).

[16] M.W. Spong, S. Hutchinson, and M. Vidyasagar. *Robot Modeling and Control*. 2nd. Wiley, 2020.

[17] Paul Allen Tipler and Gene Mosca. *Physics for Scientists and Engineers: Mechanics,*

Oscillations and Waves, Thermodynamics. 6th ed. Vol. 1. Rio de Janeiro: LTC, 2009.

[18] Unity Technologies. *ROS-TCP-Connector*. https://github.com/Unity-Technologies/ROS-TCP-Connector. Accessed: 2025-06-30. 2024.

[19] J. Yuh. "Design and Control of Autonomous Underwater Robots: A Survey". In: *Autonomous Robots* 8.1 (2000), pp. 7–24.

APPENDIX A
MECHANICAL TEST PLAN

D. Leakage Tests

To ensure the submarine's hulls were watertight, three types of leak tests were performed. First, a negative pressure test was conducted, removing air from the hull and verifying that the internal pressure remained stable over time outside of water. The second test consisted of submerging the hulls underwater, sealed at atmospheric pressure, and checking for water ingress. Finally, in the third test, the hulls were submerged underwater, and positive pressure was injected to identify more subtle leaks through the release of bubbles.

E. Pre-fabrication Simulations

To ensure the parts could withstand the pressures expected for their use, static pressure simulations were performed in Autodesk Fusion under various pressure scenarios with different component versions to minimize production costs.

F. CFD simulations

After the AUV was build, including both primary structure and its fairing, CFD simulations were performed using the software ANSYS Fluent, through its student license, mainly to verify the development of hydrodynamic forces external to Peixonauta's body. Results were concatenated in some graphs using SciDavis, and the following conclusions were taken:

- As expected, both lift and drag coefficients stayed near the average value, validating the study around those (fig 3);

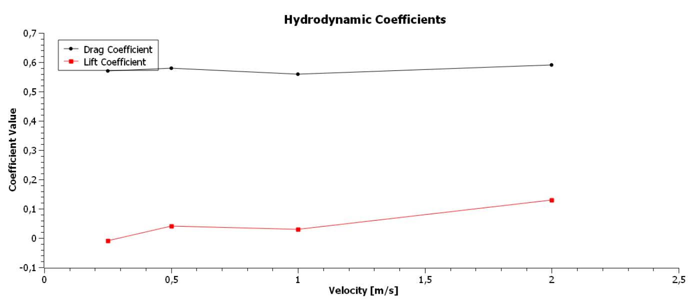

Fig. 3. Coefficient X Velocity

- The AUV geometry is sufficiently smooth for low velocities under 1.5m/s, which satisfies the value range proposed for its real working state (fig 4);

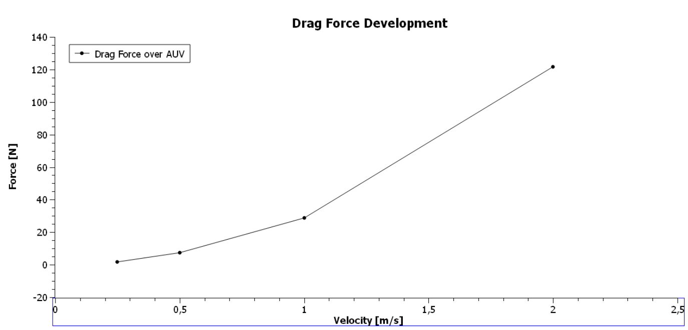

Fig. 4. Drag Force X Velocity

- Although the values were enough for what is intended, velocities over that mark shows that minimal details need to be improved in order to guarantee efficiency in other situations;
- Also, with the limitations imposed by Student License, results were somehow influenced by reductions in mesh refinement (5).

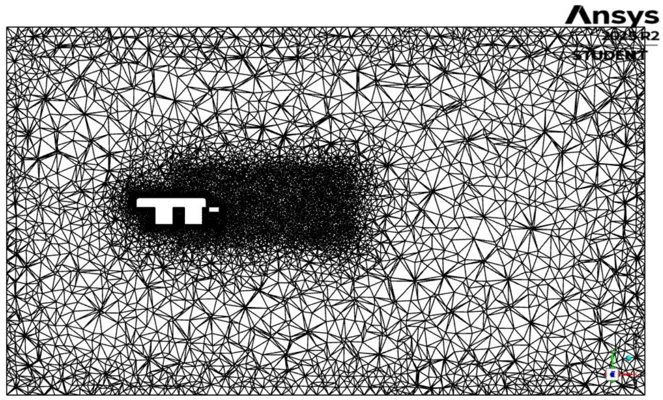

Fig. 5. Mesh

APPENDIX B
SOFTWARE TEST PLAN

This development cycle prioritized design refinement and expanded system validation relative to the previous year. The testing methodology was structured in two sequential phases: first, verification of fundamental vehicle functionality in Remotely Operated Vehicle (ROV) mode — covering motor actuation, control strategy, camera integration, and hydrodynamic behaviour — and second, validation of autonomous operation through the mission planning stack implemented via a dedicated Behaviour Tree (BT).

ROV Validation

1) Motor Actuation: A motor actuation test was conducted in open-loop configuration to verify the correct and independent operation of all seven thrusters. Each thruster was commanded individually to confirm rotational direction, absence of mechanical interference, and electrical continuity prior to closed-loop testing.

2) Virtual Validation: Prior to physical trials, the complete software stack was validated within the updated Unity 6 simulation environment. This step allowed identification and correction of implementation faults in control logic, sensor integration, and inter-node communication, providing confidence that the software design performed as specified before exposure to uncontrolled physical conditions.

3) Physical ROV Testing: Physical ROV trials were conducted at the Centro Olímpico pool, Universidade de Brasília (UnB). These trials evaluated hydrodynamic behaviour, thruster response under realistic buoyancy and drag conditions, and watertight integrity of all hull penetrations. Following minor corrective adjustments to both software parameters and mechanical components, full ROV functionality was confirmed.

Autonomous Operation Validation

4) Behaviour Tree Integration: The mission planning stack for the RoboSub 2026 competition was implemented through a BT architecture integrated with the primary ROS functional nodes, GOTO and ALIGN, for instance, which in turn interface with the Visual Servoing and Object Avoidance subsystems. Integration testing verified correct node intercommunication and expected behavioural sequencing across representative mission segments.

5) Full Competition Simulation: An end-to-end simulation of the complete RoboSub 2026 task suite was executed within Unity 6, with individual scenarios constructed to emulate each task defined in the 2026 ruleset. This test constituted the primary integration validation of the full software stack, simultaneously exercising perception, mapping, planning, control, and visual servoing under competition-representative conditions. Metrics collected during these runs informed final parameter tuning and task-specific strategy refinements.

6) Limitations: Physical autonomous trials in a competition-representative aquatic environment were not completed within the available project timeline. Consequently, complete autonomous performance in the RoboSub competition setting has been validated exclusively in simulation. This represents a known gap in the validation campaign, therefore physical autonomous testing remains the immediate priority for the period preceding the competition.